Neurocomputing 484 (2022) 149–160

Contents lists available at ScienceDirect

Neurocomputing

journal homepage: www.elsevier.com/locate/neucom

Analysis of reliable deployment of TDOA local positioning architectures

Javier Díez-González *, Rubén Álvarez *, Paula Verde, Rubén Ferrero-Guillén, Hilde Perez

Department of Mechanical, Computer and Aerospace Engineering, Universidad de León, 24071 León, Spain

ARTICLE INFO

Article history:
Received 20 February 2021
Revised 28 November 2021
Accepted 27 December 2021
Available online 30 December 2021

Keywords:
A-TDOA
Cramèr-Rao bounds
Localization
Local positioning systems
Optimization
Sensor failure
TDOA
Wireless sensor networks

ABSTRACT

Local Positioning Systems (LPS) are supposing an attractive research topic over the last few years. LPS are ad-hoc deployments of wireless sensor networks for particularly adapt to the environment characteristics in harsh environments. Among LPS, those based on temporal measurements stand out for their trade-off among accuracy, robustness and costs. But, regardless the LPS architecture considered, an optimization of the sensor distribution is required for achieving competitive results. Recent studies have shown that under optimized node distributions, time-based LPS cumulate the bigger error bounds due to synchronization errors. Consequently, asynchronous architectures such as Asynchronous Time Difference of Arrival (A-TDOA) have been recently proposed. However, the A-TDOA architecture supposes the concentration of the time measurement in a single clock of a coordinator sensor making this architecture less versatile. In this paper, we present an optimization methodology for overcoming the drawbacks of the A-TDOA architecture in nominal and failure conditions with regards to the synchronous TDOA. Results show that this optimization strategy allows the reduction of the uncertainties in the target location by 79% and 89.5% and the enhancement of the convergence properties by 86% and 33% of the A-TDOA architecture with regards to the TDOA synchronous architecture in two different application scenarios. In addition, maximum convergence points are more easily found in the A-TDOA in both configurations concluding the benefits of this architecture in LPS high-demanded applications.

1. Introduction

The recent development of increasingly complex technological activities has supposed growing accuracy localization needs for the proper performance of tasks such as autonomous vehicles, surveillance, Unmanned Aerial Vehicles (UAV) low-level flights or robot indoor navigation. The high accuracy required for these sorts of applications has entailed the interest in Local Positioning Systems (LPS) where the positioning signal travels reduced paths among the target and the architecture sensors. This fact enables the reduction of the LPS noise and clock uncertainties with regards to Global Navigation Satellite Systems (GNSS) due to the ad-hoc deployment of sensors of LPS which particularly fit the environmental characteristics where these systems are deployed.

Therefore, LPS cover a defined and known space with architecture sensors maximizing beneficial properties for the wireless sensor networks such as coverage, uncertainties reduction, failure enhancements, obstacle adaptability or energy constraints [1]. LPS are classified through the physical property measured for determining the target location: time [2], power [3], frequency [4], angle [5], phase [6] or combinations of them [7].

Among LPS, time-based localization is the most extended due to their reliability, stability, robustness, easy-to-implement hardware architectures and cost-effective deployments [8]. Time-based positioning systems rely on the measurement of the total or relative travel time of the positioning signals from the target to the receivers generating two different system conceptions: total time-of-flight- Time of Arrival (TOA) [9]- and relative time-of-flight -Time Difference of Arrival (TDOA) [10] systems-.

TOA systems are based on the measurement of the complete time from the emission of the positioning signal until its reception in the architecture sensors. This methodology allows the definition of a sphere of possible target locations for each of the measurements computed. It requires the synchronization of the clocks of all the system sensors to compute both the timestamp of the emission and the instant of reception of the positioning signal [11]. The signal processing to calculate the target location needs at least four different receivers to unequivocally define the target in 3D applications through the intersection of the spheres generated.

TDOA systems compute the relative time lapse between the reception of the positioning signal in two different receivers. Hence, the synchronization of the TDOA architectures is optional.

* Corresponding authors.
E-mail addresses: jdieg@unileon.es (J. Díez-González), ralvf@unileon.es (R. Álvarez).

https://doi.org/10.1016/j.neucom.2021.12.074
0925-2312/

Two main configurations are distinguished in TDOA localization: synchronous TDOA (i.e. the architecture sensors are all synchronized) and Asynchronous TDOA (A-TDOA). A-TDOA architecture achieves the independence from the synchronization of the sensor clocks through the centralization of the time measurements in a single clock of a coordinator sensor (CS) [12] through a receive and retransmit strategy.

Time synchronization has been demonstrated to act as a relevant factor in the uncertainties of LPS applications [13] thus showing the A-TDOA architecture a better adaptation to these contexts. However, the consideration of a CS where the time measurements are collected, makes the A-TDOA be dependent on the CS and possible failures in these sensors requires a pre-defined strategy to guarantee the system availability in those fatal cases [8]. In addition, the necessity of assuming that at least one CS of the architecture must be linked with all the coverage region of the LPS reduces the versatility of the A-TDOA deployment of the CS which is not a restriction for the TDOA synchronous architecture. This is especially relevant in harsh application environments. Therefore, no a priori suitable architecture can be defined for a particular LPS application and the two TDOA configurations must be considered to adequately define the more promising architecture examining the environment of application characteristics and the potential disadvantages of each architecture.

Another important issue for the comparison among the TDOA architectures is the position calculation algorithms which also have relation with the architecture deployments. TDOA measurements lead to hyperboloid surfaces of possible location of targets. Each measurement involves two different architecture sensors which allows the obtention of a hyperboloid equation. Nevertheless, among the set of measurements, only (n-1) independent equations are achieved from n different sensors [14]. The required number of sensors to unequivocally determine the target position is 5 sensors for three-dimensional applications. However, the intersection of three different hyperboloids (4 sensors) in TDOA systems allows the obtention of two different potential solutions. Nevertheless, these solutions are not able to be discarded from a mathematical point of view.

In one of our recent studies [15], we have demonstrated that a reliable unique solution to the intersection of three hyperboloids or spheres can be selected through the maximization in the entire coverage region of the distance between the two potential solutions by means of Genetic Algorithms (GA). We achieve this result by applying Taylor-Based algorithms [16] from an initial iteration point which must be close enough to the final solution.

However, the attainment of the minimum number of sensor nodes in coverage for calculating the target location is not enough condition to guarantee the algorithm convergence. The iterative method requires an initial position for the iterations which must be close enough to the target location in order to find the target position. This is due to the elimination of the residuals of the Taylor-Based algorithm which allows to linearize the localization problem only if there is not much distance from the initial iteration point to the target location [17].

Nonetheless there is not a pre-defined distance from which the initial iteration point can always make the algorithm converge. This is due to the properties of the intersection of the hyperboloids involved in the position calculation. Consequently, we defined in [15] a convergence radius from which any inside point can guarantee the convergence to the centre of the sphere (i.e. the target location). The maximization of the convergence radius in the entire coverage region favours the safety application of the Taylor-Based algorithm thus securing the availability of the LPS [18]. But, not an initial point so close to the final target location can be always found (e.g. the fist iteration point of the time series or in some regions in which attaining high convergence radius is roughly difficult).

Therefore, a methodology to secure the position determination in those cases must be proposed in order to make the system available in these adverse conditions. In this paper, we introduce for the first time in the authors' best knowledge the maximum convergence points to solve this problem in TDOA Taylor-Based positioning calculations. Maximum convergence points are defined as spatial points from which the convergence to any possible target location in coverage can be guaranteed. These points must be pre-defined through a priori knowledge and its application in practical cases is done through the employment of the maximum convergence point which is closer to the architecture sensors which have received the positioning signal thus achieving a faster convergence of the positioning algorithm which is critical in real-time navigation.

Node deployment has shown direct impact both for the achievement of the position disambiguation and for the definition of maximum convergence points. Therefore, a methodology to find an optimized sensor distribution in both TDOA architectures is proposed in this paper in order to compare the availability properties of each architecture.

The sensor deployment is also related to the localization error of the LPS architecture. Cramèr-Rao Lower Bound (CRLB) [19,20] derivations allow the characterization of the system uncertainties, thus estimating the minimum achievable error in positioning systems [21]. This has allowed us to study the node deployment optimization, known as the Node Location Problem (NLP) [22], in TDOA architectures by means of GA [23,24]. The reason of the use of metaheuristic methodologies relies on the NP-Hard problem solution of the 3D sensor deployment in LPS [25] and consequently many different approaches have been proposed in the literature [26,27].

This problem has also shown the impossibility of making a joint derivation of the CRLB for the entire coverage region of the LPS deployed [28]. This reason has also motivated the employment of heuristic methodologies for finding optimal sensor distributions. The CRLB model for the consideration of the quality of a node distribution is considering in this paper both a characterization of the noise of the communications channel and the uncertainties of the temporal measurements in the system clocks as we introduced in [29].

In this paper, we propose a GA optimization for the 3D node deployment of the TDOA positioning architectures (i.e. synchronous TDOA and A-TDOA) with five architecture sensors (i.e. the minimum required number of sensors to unequivocally determine the target location) in order to analyse and compare the reliable deployment of these architecture in LPS applications. The reliability of the architectures is guaranteed through the optimization of the sensor distribution to enhance the architecture properties in failure conditions of some of the sensor nodes. This supposes the maximization of the radius of convergence in the entire target coverage region of the system both in nominal and failure conditions, the definition of maximum convergence points to attain the convergence of the Taylor-Based algorithm in harsh locations and for the initial iteration point in the connection of the target to the localization architecture and the reduction of the system uncertainties in nominal and failure conditions through the CRLB.

The remainder of the paper is organized as follows: a revision of the state-of-art of the Node Location Problem in LPS is presented in Section 2, the definition of the optimization problem is analysed in Section 3, the algorithm for the target unequivocal location determination in TDOA systems and the proposition of the maximum convergence points are introduced in Section 4, the CRLB model for the quantification of the noise and clock uncertainties of the synchronous and asynchronous TDOA architectures is shown in Section 5, the GA optimization and the fitness functions of each architecture are detailed in Section 6 and Sections 7 and 8 show the results and conclusions of the present paper.

2. Node location problem

The Node Location Problem (NLP) is defined as the finding of the optimal Cartesian coordinates of the architecture sensors of the wireless local networks [30]. It entails the coverage problem in communications networks [31] and it adds the reduction of the system uncertainties in localization networks [32]. Both have been categorized as NP-Hard [25], therefore the localization NLP supposes a challenge for finding optimal solutions in reasonable time.

In addition, the dimensions of the space of solutions of the NLP promotes the discretization of the space in which the sensors can be located (i.e. Node Location Environment (NLE) [33]). However, this discretization must preserve sufficient representativeness of the space of solutions for finding acceptable results. Moreover, low discretization values are not only necessary for the location of the sensor nodes but also for the coverage region of the LPS. The coverage of every eventual location of a target (i.e. Target Location Environment (TLE) [23]) must be considered together with the minimization of the system uncertainties in every TLE point. The consideration of the uncertainties in the entire TLE cannot be jointly derived [28] which makes the NLP be a combinatorial non-derivable problem. Therefore, it cannot be addressed through derivative direct methods and the discretization of the TLE is also a requirement in NLP optimization. The discretization of the TLE must be sufficient to represent the properties of the target in the entire coverage region, thus requiring an exhaustive analysis of all the space within this region.

The double deep space discretization both for the NLE and for the TLE promotes the exploration of a huge space of solution in the decision variables (i.e. the spatial coordinates of the sensors) due to the NLE discretization with considerable computational cost in the definition of the quality of the node distribution due to the TLE discretization and due to the characteristics of the cost function.

Therefore, the exact methods (i.e. exploring every possible combination of sensors in space) are only utilized in reduced environments (i.e. low discretization values) with few sensors [34] since the complexity is factorial with the number of nodes [35]. Approximation algorithms are employed in more refined optimizations for obtaining promising solutions in reduced time [36]. But, generally, the complexity of the problem suggests the usage of metaheuristics for the solution of the NLP.

Simulated annealing [37], the salp swarm algorithm [38], memetic algorithms [39,40], the dolphin swarm algorithm [41], bacterial foraging algorithm [42], the grey wolf optimization [43], differential evolution [44] or elephant herding optimization [45] have been proposed for the NLP but especially the GA have been used due to their excellent trade-off between exploration and exploitation of the space of solutions [46,47,48].

The GA also allows a more sophisticated control through the hyperparameters over the optimization process which is crucial for dealing with huge spaces of solutions in which the diversification is critical. For this reason, we select the GA for this paper since we are dealing with an optimization of the sensor distribution which deals with a combination of uncertainties and positioning algorithm enhancements which has not been addressed before in the literature.

While the reduction of the noise uncertainties due to the spatial location of the nodes through the CRLB has been previously presented in [23], we later extended this analysis by considering the time measurement uncertainties in the system clocks in [29]. In this paper, we extend these works through the consideration of possible sensor failures in the architecture nodes proposing a versatile optimization which considers both nominal and failure situations of the performance of the LPS TDOA architectures. In addition, we introduce a methodology for guaranteeing the positioning algorithm convergence through the maximization of the radius of convergence for both nominal and failure conditions. We finally enhance the global convergence properties of the entire TLE region through the finding of maximum convergence points in the optimization.

This methodology allows us in this paper to compare the versatility and reliability of the TDOA positioning architecture in a real 3-D application environment extracting valid conclusions for the localization community.

3. Problem definition

The NLP entails the definition of the optimal Cartesian coordinates of the sensor nodes of the wireless sensor network architecture in order to maximize the design objectives of the system network.

Mathematically, it is the exploration inside the set (S) containing every possible combination of sensors in space in order to find the subset (S_i) with the spatial coordinates of all the architecture sensors (n_s). This subset is composed by an array ($\langle S_i \rangle = \langle s_1, \cdots, s_{n_s} \rangle$) with the Cartesian coordinates of any sensor ($\langle s_i \rangle = \langle x_i, y_i, z_i \rangle$).

Therefore, the optimization of the NLP particularized for this paper objectives follows a maximization equation (Eq. (1)) which considers the accuracy of the localization architecture in nominal and failure conditions, the convergence properties of the Taylor-Based algorithm to determine the target location, the achievement of maximum convergence points in the coverage region and the penalizations for not attaining the constraints of the optimization:

$$Maximize\ Z = ff\left(ff_{CRLB_N}, ff_{CRLB_F}, ff_{CONV_N}, ff_{CONV_F}, ff_{MCP_N}, ff_{MCP_F}, ff_{pen}\right) \quad (1)$$

where $ff_{CRLB_N}, ff_{CRLB_F}, ff_{CONV_N}, ff_{CONV_F}, ff_{MCP_N}, ff_{MCP_F}, ff_{pen}$ are the fitness function depending on the CRLB in nominal and failure conditions, the fitness function considering the convergence properties of the Taylor-Based localization algorithm in nominal and failure conditions and the fitness function for the determination of the maximum convergence points that we first introduce in this paper and the penalizations for the architectures in which some sensors are occupying banned regions respectively

This proposed optimization must consider some restrictions for ensuring the performance of the localization architecture in every eventual condition in the whole coverage region. For this purpose, we must include some optimization constraints for allowing only valid combinations of sensor locations in space (sensor distribution constraints), some restrictions for achieving the effective coverage in all the space covered by the localization sensor network allowing the position calculation in the entire TLE (coverage constraints) and some constraints for ensuring the proper functioning of the localization algorithm in both nominal and failure conditions (algorithm constraints).

The restrictions for attaining valid distributions of sensors in space are designed in order to perform the metaheuristic search in the set of potential locations for the sensors (S_i) assuring that each of the sensors deployed of the architecture (s_i) are located in valid spatial locations avoiding potential positions that are prohibited in the terrain due to obstacles. These invalid locations are included in the subset U formalizing the sensor distribution constraints as:

$$x_{lim_1} \le x_i \le x_{lim_2} \quad \forall x_i \in s_i; s_i \in S_i; s_i \notin U \tag{2}$$

$$y_{lim_1} \le y_i \le y_{lim_2} \quad \forall y_i \in s_i; s_i \in S_i; s_i \notin U \tag{3}$$

$$z_{lim_1} \le z_i \le z_{lim_2} \quad \forall z_i \in s_i; s_i \in S_i; s_i \notin U \tag{4}$$

wherex_{lim_1},x_{lim_2},y_{lim_1},y_{lim_2}, $z_{lim_1}$and z_{lim_2} the lower and upper bounds for the location of the sensors in the simulations environment; U the subset containing the forbidden regions for the location of the sensors in the environment.

The coverage constraints are related to guarantee the reception of an effective signal in the architecture sensors to compute the time measurements. This is achieved when the signal-to-noise ratio in the signal received in the architecture sensors exceeds a threshold. Since the TDOA and the A-TDOA architectures have different connections among the system devices due to the necessity for the A-TDOA architecture of collecting all the time measurements for determining the target location, the effective coverage of a particular worker sensor in the A-TDOA architecture must guarantee not only the effective link to the target as in the TDOA architecture but also must guarantee exceeding the threshold in its connection with the CS. In addition, more than the minimum number of receivers to calculate the position in both localization architectures must receive an effective signal to be able to determine the localization of the target. All these coverage constraints for the optimization are presented hereafter:

$$cov_k \ge n_{min_{TDOA}} \quad \forall k \in K_{TLE} \tag{5}$$

$$cov_k = \sum_{i=1}^{n_s} cov_{ki} \tag{6}$$

$$cov_{ki_{TDOA}} = \begin{cases} 1 & if\ SNR_{ki} \ge SNR_{threshold} \\ 0 & otherwise \end{cases} \tag{7}$$

$$cov_{ki_{A-TDOA}} = \begin{cases} 1 & if (SNR_{ki} \ge SNR_{threshold})\ and\ (SNR_{ij} \ge SNR_{threshold}) \\ 0 & otherwise \end{cases} \tag{8}$$

$$cov_{CS_k} \ge 1 \quad \forall k \in k_{TLE} \tag{9}$$

$$cov_{CS_k} = \sum_{j=1}^{n_{cs}} cov_{CS_{kj}} \tag{10}$$

$$cov_{CS_{kj}} = \begin{cases} 1 & ifSNR_{kCS_j} \ge SNR_{threshold} \\ 0 & otherwise \end{cases} \tag{11}$$

where cov_k represents the number of sensors under effective coverage in a particular discretized point of the TLE k; $n_{min_{TDOA}}$ is the minimum number of architecture sensors in coverage to be able to calculate the target location in the TDOA architecture that we demonstrated in [15] to be set to four; K_{TLE} are the total number of discretized points in the TLE region; cov_{ki} is the definition of the effective coverage of a determined sensor i of the architecture deployed; SNR_{ki} is the signal-to-noise ratio received in the architecture sensor i from the emission of the positioning signal from the point k of the TLE discretized region which must exceed the $SNR_{threshold}$ to consider an effective coverage; SNR_{ij} is the signal-to-noise ratio of the link between the worker sensor i and the coordinator sensor j in the architecture A-TDOA; cov_{CS_k} are the number of CS under effective coverage which must be at least one to be able to determine the target location; $cov_{CS_{kj}}$ is the definition of the effective coverage of the CS j in the discretized point SNR_{kCS_j} is the signal-to-noise ratio in the reception of the positioning signal in the CS j from the target in point k.

Finally, some restrictions are required for allowing the correct performance of the Taylor-Based positioning algorithm proposed in this paper. First, we propose a threshold radio of convergence which allows the successive calculation of the target location with a reasonable refresh rate and the existence of at least a maximum convergence point to ensure the positioning calculation in eventual harsh conditions:

$$R_{conv k} \ge R_{threshold} \quad \forall k \in k_{TLE} \tag{12}$$

$$n_{MCP} \ge 1 \tag{13}$$

where $R_{threshold}$ is the minimum distance from which the position calculation can be effectuated in the entire TLE to consider the full availability of the TDOA architecture under evaluation and n_{MCP} is the number of maximum convergence points in the coverage region of the architecture.

4. Taylor-based localization algorithm

Relative time measurements in TDOA systems lead to hyperboloid equations of possible target locations. Numerical methods are needed to solve the intersection of these non-linear equations. Taylor-Based algorithms in TDOA systems allow the linearization of the equations of the time difference of arrival of the positioning signal to two different architecture sensors:

$$\begin{aligned} R_{ij} = d_{ij} = d_{Ei} - d_{Ej} = ct_{ij} = c(t_i - t_j) \\ = \sqrt{(x_E - x_i)^2 + (y_E - y_i)^2 + (z_E - z_i)^2} \\ - \sqrt{(x_E - x_j)^2 + (y_E - y_j)^2 + (z_E - z_j)^2} \end{aligned} \tag{14}$$

where R_{ij} and d_{ij} represent the distance difference of the signal travel from the emitter to the architecture sensors$i$ and j, $d_{Ei}$and d_{Ej} are the total distance from the emitter (E) to the system sensors i and j, c is the speed of the radioelectric waves, t_{ij} is the time difference of arrival measured in the architecture sensors,t_i and $t_j$is the total time of flight of the positioning signal from emitter to receivers i and$j$ respectively and (x_E, y_E, z_E), (x_i, y_i, z_i) and $(x_j, y_j, z_j)$are the Cartesian coordinates of the target and the sensors i and$j$.

Taylor approximation truncated on first order is applied in Eq. (14) to linearize the equation from an initial iteration point (x_0, y_0, z_0):

$$R_{ij} = ct_{ij} = R_{ij_0} + \frac{\partial R_{ij}}{\partial x}\Delta x + \frac{\partial R_{ij}}{\partial y}\Delta y + \frac{\partial R_{ij}}{\partial z}\Delta z \tag{15}$$

where R_{ij_0} is the range difference of arrival in the initial iteration point, $\frac{\partial R_{ij}}{\partial x}$, $\frac{\partial R_{ij}}{\partial y}$and $\frac{\partial R_{ij}}{\partial z}$ are the partial derivatives of the range differences measured in the i and j architecture sensors particularized in the initial iteration point. The application of Eq. (15) to every pair of sensors of the TDOA architecture leads to the following relation, that enables the obtainment of the target location.

$$\Delta P = (H^t H)^{-1} H^t \Delta R = \begin{pmatrix} \Delta x \\ \Delta y \\ \Delta z \end{pmatrix} \tag{16}$$

where H is the partial derivative matrix, andΔP represents the incremental values from the last iteration point in each space direction which supposes the unknown of the equation.

This method is able to calculate the target location through the least squares Taylor-Based algorithm proposed in this section. However, it relies on the definition of a close point to the final target position to start the iterative method in order to define the ΔP values to sequentially update the position until no changes in the iterative process are observed.

Therefore, far away starting positions to the final target location could produce unstable target position calculations due to the high values of the residuals of the Taylor approximation of Eq. (15). Thus, convergence problems in the algorithm could produce architecture unavailability.

In this paper, we propose two different methods to deal with this potential problem: the radius of convergence and the definition of maximum convergence points.

The radius of convergence is the maximum distance from which the initial iteration point can assume the convergence of the algorithm. It requires the definition of a theoretical sphere around the target real location which must be a priori maximize to enhance the availability properties of the Taylor-Based localization algorithm.

For locating services, depending on the refresh rate of the positioning calculation determination and the maximum speed of the targets to locate, a threshold on the radius of convergence ($R_{threshold}$) for guaranteeing the convergence of the positioning algorithm is obtained. In this sense, safe operating conditions are ensured when all TLE point present a convergence radius that exceed the $R_{threshold}$.

The maximum convergence points (n_{MCP}) are the TLE points of the space which can convergence to any TLE discretized point of the architecture. The definition of these points may help the localization algorithm in divergence-detected cases and for the initial target location determination of the time series.

The maximum convergence points also support the system operation in harsh environments in which the attainment of high radius of convergence values is not possible. However, the closer the initial iteration point the faster the convergence of the algorithm which is critical for real-time LPS applications. Therefore, the greater number of maximum convergence points the more robustness for the TDOA architecture. However, not every simulation scenario can define a maximum convergence point and a combination of pre-defined points can assure the convergence of the architecture.

For this reason, a maximum convergence point can be a unique discretized point of the space (i.e. the ideal case) or a combination of points.

Mathematically, an ideal unique maximum convergence point is defined as:

$$n_{MCP_i} = \begin{cases} 1 & if\ TLE_{CONV_i} = K_{TLE} \\ 0 & otherwise \end{cases} \tag{17}$$

$$TLE_{CONV_i} = \sum_{k=1}^{K_{TLE}} TLE_{CONV_{ik}} \tag{18}$$

$$TLE_{CONV_{ik}} = \begin{cases} 1 & if\ i\ converge\ to\ k \\ 0 & otherwise \end{cases} \tag{19}$$

where n_{MCP_i} refers to the definition of a maximum convergence point in the space location i; TLE_{CONV_i} is the number of the discretized points of the TLE to which the point i can convergence which must be equal to the total K_{TLE} in order to define a maximum convergence point, and $TLE_{CONV_{ik}}$ defines if the point i can guarantee convergence to the point k of the discretized TLE points.

5. CRLB estimation for TDOA and A-TDOA architectures

Errors during time measurements produce uncertainties that affect the performance in terms of accuracy and stability of the localization architectures. The CRLB provides the maximum attainable accuracy for each operating condition, i.e. depending on the characteristics and magnitudes of the time measurement errors. Its large-scale application in the positioning field [49,50] just as their capability of adaptation to several error models, support their application to the NLP problem in complex heteroscedastic environments [51].

Recent studies [51] have proposed a matrix form for the CRLB in terms of the Fisher Information Matrix (FIM) which allows the definition of the uncertainties models in the covariance matrix of the system:

$$FIM_{mn} = \left(\frac{\partial h(TS)}{\partial TS_m}\right)^T R^{-1}(TS)\left(\frac{\partial h(TS)}{\partial TS_n}\right) + \frac{1}{2} tr\left\{R^{-1}(TS)\left(\frac{\partial R(TS)}{\partial TS_m}\right)R^{-1}(TS)\left(\frac{\partial R(TS)}{\partial TS_n}\right)\right\} \tag{20}$$

where m and n are the sub-indexes of the FIM matrix for the estimation, TS represents the location of the target sensor expressed by their Cartesian coordinates, $h(TS)$ contains the characterization of the deployed positioning architecture represented by the travel of their signals, expressed for TDOA and A-TDOA systems through the following relations:

$$h_{TDOA_i} = \|TS - CS_i\| - \|TS - CS_j\|$$

$$i = 1, \cdots, N_{cs};\ j = 1, \cdots, N_{CS};\ i \neq j \tag{21}$$

$$h_{A-TDOA_i} = \|TS - WS_i\| + \|TS - CS\| - \|WS_i - CS\|$$

$$i = 1, \cdots, N_{ws} \tag{22}$$

where CS and WS are related to the Coordinator and Worker Sensors respectively, N_{CS} is the number of CS, N_{WS} the number of WS, $R(TS)$ is the covariance matrix that enclosures the heteroscedastic probability distributions of the time measurements errors of the system. Under this consideration, noise uncertainties are modeled through a Log-Normal path loss model for wireless positioning signals. Clock errors are implemented in the variances of each time measurement (T) by their initial-time offset (U), time from last synchronization (T_0)and clock drift (η) of their devices.

Noise and clock errors can be considered independent since the causes of their appearance are different. Noise uncertainties are promoted by the degradation of the positioning signal in its travel to the architecture sensor in TDOA architectures adding the transmission from the WS to the CS in A-TDOA architectures. Clock errors are due to the characteristics of the system clocks in charge of the time measurements and the protocol for the synchronization of the system devices. Their stochastic nature recommends performing a Monte-Carlo model for estimating its value for each one of the time measurements needed to calculate the target location.

Particularly, TDOA signal noise depends on the two required transmissions i and j for collecting a time measurement for which we apply the Log-Normal path loss model and the time measurement of these two signals in the architecture sensors i and j generate two different probabilistic distributions for the clock errors depending on the initial time-offset, the time from the last synchronization, the clock drift and the truncation error.

Regarding the A-TDOA architecture, the modeling of the noise uncertainties must also consider the path losses from the WS to the CS and the clock error model eliminates the terms of the synchronization error and reduces to a unique Monte-Carlo simulation for each time measurement since this architecture only collects a time measurement for each hyperbolic equation in the CS.

Therefore, the TDOA architecture reduces the noise uncertainties with regards to the A-TDOA architecture since their positioning signal paths are shorter, but A-TDOA architecture provides lower clock errors which do not allow us to conclude that any of the architectures overcomes the other in any localization context. This complete model for the estimation of the system uncertainties

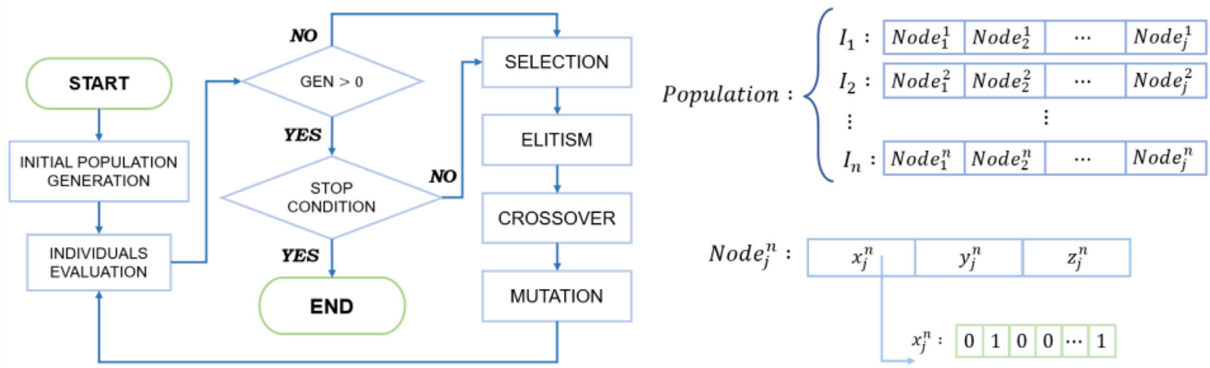

Fig. 1. Flux diagram of the GA and the proposed genotypes codification. All node positions are scaled to cartesian coordinates within the delimited regions.

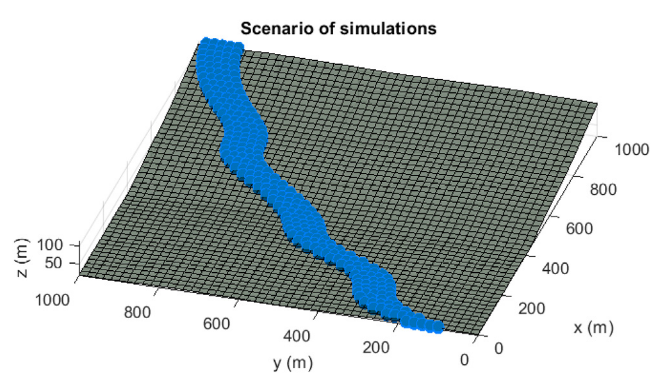

Fig. 2. The scenario of simulations. Base surface is characterized through grey colors, while TLE region is depicted in blue color.

Table 1
Configuration parameters for the TDOA and A-TDOA architectures [52,53].

Parameter	Value
Transmission power	100 W
Mean noise power	– 94 dBm
Frequency of emission	1090 MHz
Bandwidth	80 MHz
Path loss exponent	2.16
Antennae gains	Unity
Time-Frequency product	1
Clock frequency	1 GHz
Frequency-drift	$U\{-10, 10\}$ppm
Initial-time offset	$U\{15, 30\}$ns
Time from synchronization	1 µs
Architecture sensors	5

Table 2
The GA configuration [54].

GA	Settings
Population size	120
Selection technique	Tournament 2
Crossover technique	Single-point
Mutation technique	Single-point
Elitism percentage	3.5%
Mutation percentage	5%
Stop criteria	120 generations or 80% of equal individuals
Fitness function coefficients	1

was first presented in one of our recent works [29] defining the variances for the time measurements of the TDOA and A-TDOA architecture:

$$\sigma_{TDOA_{ij}}{}^2 = \frac{c^2}{B^2\left(\frac{P_T}{P_n}\right)}PL(d_0)\left[\left(\frac{d_i}{d_0}\right)^n + \left(\frac{d_j}{d_0}\right)^n\right] + \frac{1}{l}\sum_{k=1}^{l}\{|T_i - floor_{TR}(T_i + U_i - U_0 + T_0(\eta_i - \eta_0) + T_i\eta_i)|c^2\} + \frac{1}{l}\sum_{k=1}^{l}\left\{\left|T_j - floor_{TR}\left(T_j + U_j - U_0 + T_0\left(\eta_j - \eta_0\right) + T_j\eta_j\right)\right|c^2\right\} \quad (23)$$

$$d_i = \|TS - CS_i\|$$

$$d_j = \|TS - CS_j\|$$

$$i = 1, \cdots, N_{CS}$$

$$j = 1, \cdots, N_{CS}$$

$$where\ i \neq j$$

$$\sigma^2_{A-TDOA_i} = \frac{c^2}{B^2\frac{P_T}{P_n}}PL(d_0)\left[\left(\frac{d_i}{d_0}\right)^n + \left(\frac{d_{TS}}{d_0}\right)^n + \left(\frac{d_{CS}}{d_0}\right)^n\right] + \frac{1}{l}\sum_{k=1}^{l}\{|(T_i + T_{TS} - T_{cs}) - floor_{TR}[T_i + T_{TS} - T_{CS})(1 + \eta_{CS})]|c^2\} \quad (24)$$

$$d_i = \|TS - WS_i\|$$

$$d_{TS} = \|TS - CS\|$$

$$d_{CS_i} = \|WS_i - CS\|$$

$$i = 1, \cdots, N_{WS}$$

where c is the signal propagation speed (m/s), B is the signal bandwidth (Hz), Pt is the power of emission (W), Pn is the mean noise level (W) obtained based on Johnson-Nyquist relation, n is the path loss exponent, d_0 depicts the reference distance for the Log-Normal model, $PL(d_0)$represents the path-loss related to the reference distance, and $floor_{TR}$ is the representation of the temporal resolution of the clocks.

Lastly, the calculation of the Root Mean Squared Error (RMSE) provides the location accuracy in terms of the sensor distribution, target location and operating conditions:

$$RMSE = \sqrt{trace\left(J^{-1}\right)} \quad (25)$$

6. GA implementation and fitness function

The performance of LPS is severely reliant on architecture sensors distributions in complex tridimensional environments. This

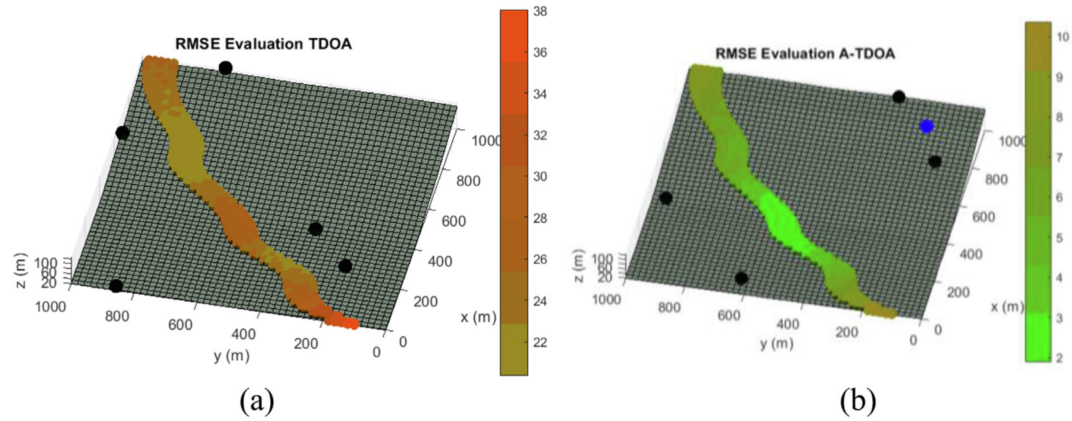

Fig. 3. CRLB estimation in meters for the TDOA and the A-TDOA systems. Black spheres represent the location of the WS and the blue sphere depicts the CS of the distribution.

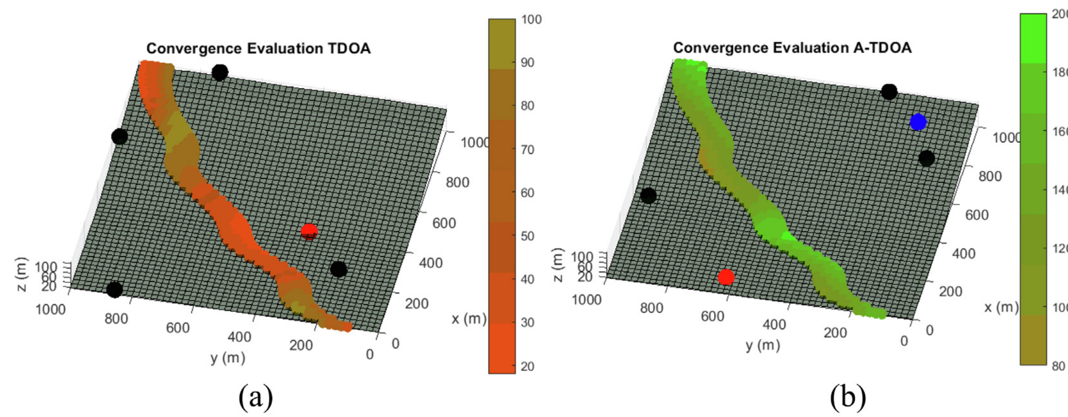

Fig. 4. Convergence evaluation in meters for the TDOA system and A-TDOA. The red sphere represents the malfunction sensor that cannot be used for position estimation.

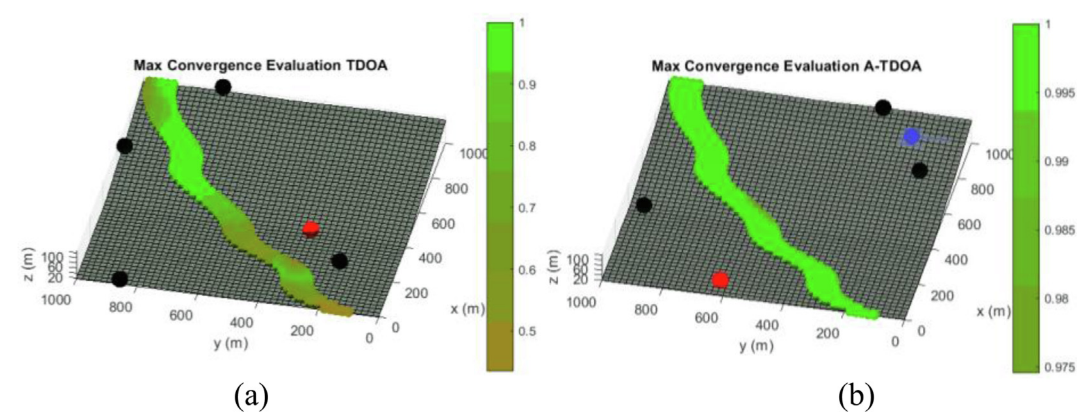

Fig. 5. Maximum convergence evaluation for $R_{threshold}$ of 200 for the TDOA system and A-TDOA system. The red sphere depicts the malfunction sensor that cannot be used for position estimation.

fact promotes that optimized sensor deployments encourage the maximization of the capabilities of the positioning systems.

Irregular 3D environments represent a complex framework for heuristic optimization techniques, due to the difficulties related to the definition and delimitation of the variables of the problem. Prior works [23], the NLP for complex scenarios with a free definition of TLE and NLE regions is solved through a scaled GA, shown in Fig. 1.

The designed codification relies on the scaled binary conversion to the real coordinates of the scenario of application, allowing total control over the spatial resolutions of NLE and TLE zones. Consequently, each individual of the population contains the cartesian

Table 3
Mean optimization results for TDOA y A-TDOA architectures in nominal and failure conditions.

Parameter		TDOA	A-TDOA
RMSE nominal (m)		25.28	5.38
RMSE failure (m)	Combination 1	46.62	–
	Combination 2	88.85	11.98
	Combination 3	55.30	13.18
	Combination 4	41.50	17.99
	Combination 5	29.05	12.57
Convergence radius nominal (m)		102.95	191.56
Convergence radius failure (m)	Combination 1	77.53	–
	Combination 2	55.34	141.55
	Combination 3	79.72	243.35
	Combination 4	68.52	214.64
	Combination 5	68.29	165.12
Max Convergence for $R_{threshold}$ = 200 nominal		0.975	1
Max Convergence for $R_{threshold}$ = 200 failure	Combination 1	0.971	–
	Combination 2	0.817	0.997
	Combination 3	0.934	1
	Combination 4	0.905	1
	Combination 5	0.959	1

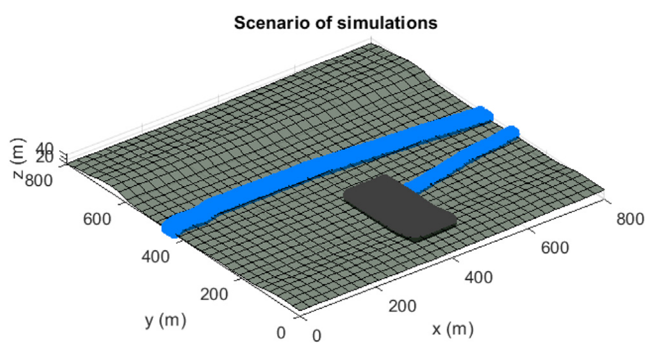

Fig. 6. The second scenario of simulations. Base surface is characterized through grey colors, in black an obstacle and TLE region is depicted in blue color.

coordinates of each sensor to be located, stored in binary, which also facilitates the implementation of multiple selection, crossover and mutation methods and different convergence criteria.

A weighted optimization is carried out for ensuring the correct maximization of accuracy and capabilities of the system in failure conditions for the TDOA and A-TDOA positioning architectures, expressed through the following relations:

$$ff = \sum_{1}^{Comb} \left\{ \frac{C_1}{K_{TLE}} \sum \left\{ \frac{\left[\left(\frac{1}{RMSE_{ref}}\right) - \left(\frac{1}{\mathbf{RMSE_{4sensors}}}\right)\right]^2}{\left(\frac{1}{RMSE_{ref}}\right)^2} \right\} + \frac{C_2}{K_{TLE}} \sum \left\{ \frac{\left[\left(\frac{1}{Dist_{ref}}\right) - \left(\frac{1}{\mathbf{Dist}}\right)\right]^2}{\left(\frac{1}{D_{ref}}\right)^2} \right\} \right\} + C_3 \sum \frac{\left\{ \frac{\left[\left(\frac{1}{RMSE_{ref}}\right) - \left(\frac{1}{\mathbf{RMSE}}\right)\right]^2}{\left(\frac{1}{RMSE_{ref}}\right)^2} \right\}}{K_{TLE}} + C_4 \sum \frac{\mathbf{MC}}{K_{MC}} - C_5 \frac{\sum_{i=1}^{N_{CS}} BL_i}{N} \quad (26)$$

where ff is the fitness function value for a specific sensor distribution, $Comb$ represents the number of possible combinations of four sensors based on the entire architectures sensors, C_k denotes the value of the k coefficient value for weighting the fitness function components, K_{TLE} is the total number of TLE points at study, $RMSE_{ref}$ and $Dist_{ref}$ depicts respectively the reference RMSE and convergence distance magnitudes for normalizing the accuracy component of the fitness function, $RMSE_{4sensors}$ is the vector that expresses the CRLB evaluation for TLE point at every combination of four sensors, $Dist$ is the vector that contains the convergence metrics for each point of the TLE zone, $RMSE$ is the accuracy evaluation for the entire TLE region using the complete architecture sensors deployment available at each place, MC represents the fulfilment of maximum convergence criteria (binary) for each TLE point, K_{MC} is the total number of analyzed situations for the maximum convergence criteria, N is the number of deployed sensors, and $BL_i$is the binary penalty associated to not allowed sensor distributions locations.

7. Results

The results for the combined optimization of accuracy, failure operation and algorithm convergence performance for TDOA and A-TDOA positioning architectures are submitted in this section. Initially, a common scenario for simulations is designed in order to enable effective comparisons between the architectures.

Based on Fig. 2, the TLE regions occupy a limited zone that extends from 0.5 to 5 m of elevation from the reference surface. This zone is discretized under a division of 20 m in the Cartesian coordinates × and y, and a spatial resolution of 1 m for the z coordinate. Under this characterization, a trade-off between processing time and continuity in solutions is accomplished for the correct evaluation of the performance of positioning systems.

The NLE expands over the entire base surface, except for the area delimited by the TLE zone. For the NLE region, the elevation of the architecture sensors is constrained in the interval [1,6] depicting a typical indoor/outdoor environment where height of sensors is limited. The spatial resolution of the NLE area is provided by the length of the chromosomes employed as individuals of the GA. For this optimization, the three Cartesian coordinates vary their resolution from 0.5 to 1 m, based on the chromosomes topology and the maximum intervals of each coordinates [23].

Tables 1 and 2 present the parameters employed for the simulations, related to the configuration of positioning systems and the setting of the GA for the optimization.

The selection of Table 1 parameters is based on the characterization of a generic technology that ensures an unbiased comparison between TDOA and A-TDOA positioning architectures. In the case of Table 2, the presented configuration of the GA provides the best trade-off between execution time and maximization of the global fitness functions, leading to optimum sensor distributions for both positioning systems.

The results of the optimization of the sensor placement of TDOA and A-TDOA architectures in the described scenario based on the predefined operating conditions and optimization methodology are presented hereafter. Fig. 3 show the RMSE evaluation for analyzed positioning systems during nominal operation.

As it can be observed in Fig. 3, A-TDOA architectures provide better performance in terms of accuracy due to the drastical reduction of location uncertainties induced by clock errors [29] in LPS.

System operation in case of malfunctions is severely limited by the convergence of the positioning algorithms implemented. Fig. 4 depict the convergence radius criteria evaluation for the TDOA and A-TDOA architectures respectively, when the minimum number of sensors is accessible for univocally calculating the location of the target.

Fig. 4 shows that the convergence radius obtained for each TLE point is larger in the case of the A-TDOA architecture, boosting the robustness of the system in failure conditions and providing higher flexibility during the operation.

Maximum convergence is analyzed based on a $R_{threshold}$ that indicates the distance to the target sensor at which the TLE inner

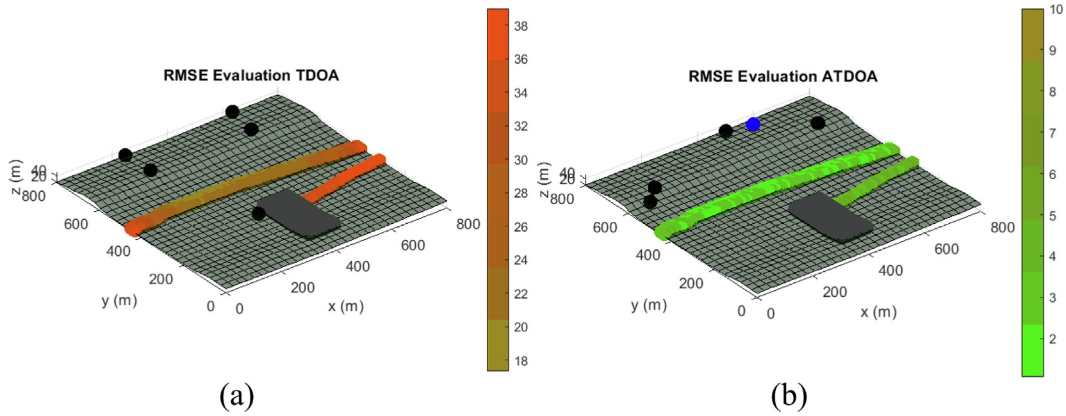

Fig. 7. RMSE evaluation for TDOA and A-TDOA architecture in a split TLE. Black spheres represent the location of the WS and the blue sphere depicts the CS of the distribution.

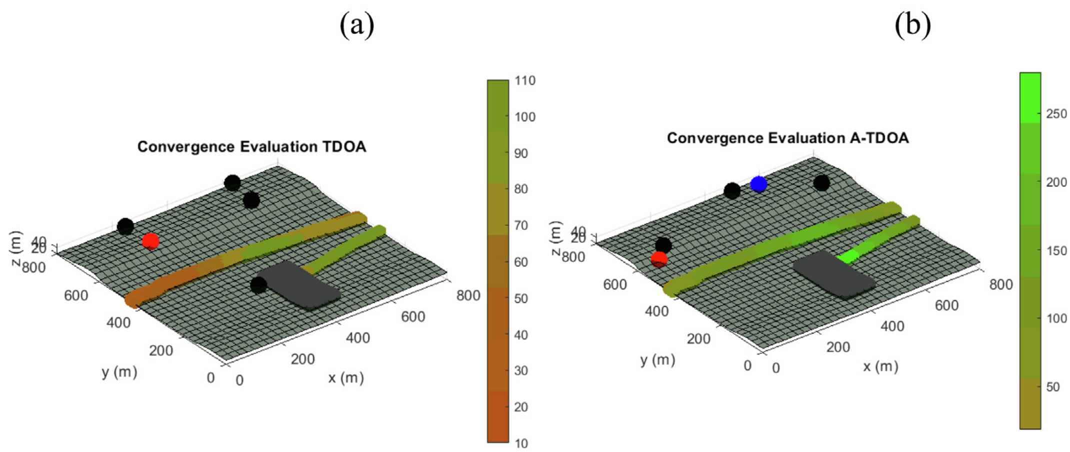

Fig. 8. Convergence evaluation in meters for the TDOA system and A-TDOA in a split TLE. The red sphere represents the malfunction sensor that cannot be used for position estimation.

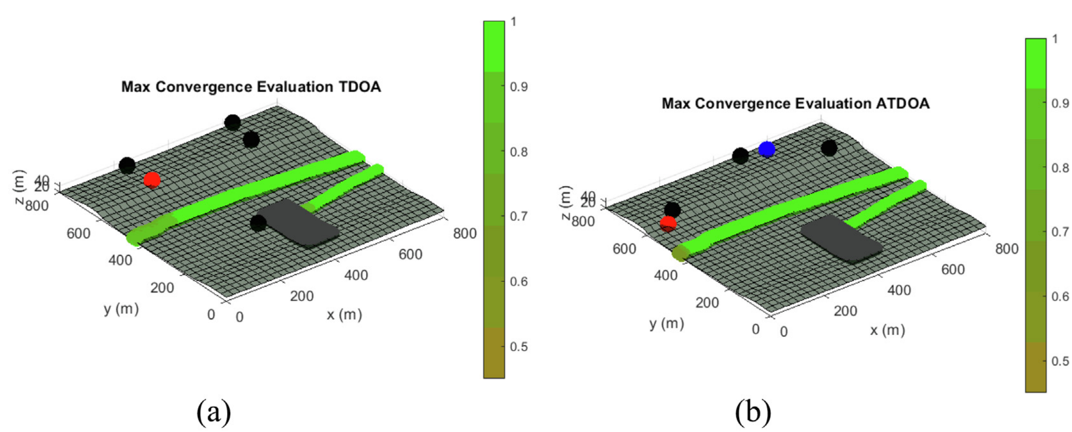

Fig. 9. Maximum convergence evaluation for $R_{threshold}$ of 200 for the TDOA system and A-TDOA system in a split TLE. The red sphere depicts the malfunction sensor that cannot be used for position estimation.

points to this radius can be used as start points to the Taylor-based iteration. Fig. 5 shows the maximum convergence evaluation in failure conditions for a $R_{threshold}$ of 200.

Lastly, Table 3 summarizes the main performance metrics related to accuracy, convergence radius, and maximum convergence capability of the positioning architectures at study, both for nominal and failure situations.

Table 3 indicates the better performance in terms of accuracy, convergence radius and maximum convergence points of the A-TDOA architecture during nominal and operating conditions. From the previous results, the reduction of 78.7% in RMSE mean values and the increase of 86% in convergence radius of the A-TDOA over the TDOA architecture must be highlighted. Also, both optimizations show that almost all points of the TLE within the $R_{threshold}$ of

Table 4
Mean optimization results for TDOA y A-TDOA architectures in a split TLE.

Parameter		TDOA	A-TDOA
RMSE nominal (m)		26.1	2.74
RMSE failure (m)	Combination 1	39.65	–
	Combination 2	36.17	9.88
	Combination 3	44.27	3.92
	Combination 4	41.89	2.95
	Combination 5	70.42	3.33
Convergence radius nominal (m)		106.32	158.65
Convergence radius failure (m)	Combination 1	56.23	–
	Combination 2	80.36	136.40
	Combination 3	110.89	136.61
	Combination 4	66.57	143.81
	Combination 5	47.48	150.42
Max Convergence for $R_{threshold}$ = 200 nominal		0.9989	0.9986
Max Convergence for $R_{threshold}$ = 200 failure	Combination 1	0.9837	–
	Combination 2	0.9702	0.9905
	Combination 3	0.9631	0.9896
	Combination 4	0.9930	0.9904
	Combination 5	0.8670	0.9906

200 are accessible for starting the Taylor-based approach for each point of the TLE region. In this sense, a great flexibility for the refreshing time of the algorithm and the speed of the target sensors is achieved, being possible to use a refreshing time of 5 s and speeds up to 140 km/h in nominal operating conditions.

Moreover, in order to validate the hypothesis that we have proposed in this paper and in order to extend the effectiveness of the results, we have included one additional scenario with different characteristics.

The scenario is composed of two independent coverage areas as it can be seen in Fig. 6.

This outdoor scenario verifies the suitability of the A-TDOA architecture where there is a main area and a secondary area representing potential rural roads. Fig. 7 shows the CRLB estimations for both architectures.

Fig. 8 shows the estimated convergence for both architectures. In this scenario, the operation of the system in case of breakdowns is not severely limited, although the TLE conditions are different and the TLE is divided. In the scenario described above, the A-TDOA architectures provide better performance.

In addition, Fig. 9 shows the comparison of the maximum convergence between the TDOA system and the A-TDOA in a scenario with two separate coverage areas.

The performance metrics obtained in this scenario are shown in Table 4. These metrics show that the A-TDOA architecture has greater precision and convergence capacity also in this second rural scenario concluding the benefits of the A-TDOA architecture in these contexts.

The previous results demonstrate that the A-TDOA architectures are suitable candidates for high-requirement LPS, when accuracy, algorithm convergence and localization system robustness are required.

8. Conclusions

Local Positioning Systems (LPS) are an active topic of research due to the development of high-demanded accurate applications such as autonomous navigation, surveillance or low-level UAV flights. LPS allow the deployment of an ad-hoc sensor distribution for adapting the characteristics of the environment in which they are deployed. This enables providing a stable and accurate localization service in harsh environments.

Among the LPS, those based on time measurements are the most extended in the literature due to their trade-off among reliability, cost, robustness and easy-to-implement hardware architectures.

The implementation of promising time-based LPS architectures requires an optimization of the node location in order to reduce the system uncertainties. This has been named as the Node Location Problem (NLP) and its fulfillment is critical for finding competitive LPS results.

Recent investigations have highlighted that after the optimization of the sensor distribution, the clock uncertainties in the time measurements represent the largest and less controllable error of the time-based LPS architectures.

Consequently, asynchronous architectures such as the Asynchronous Time Difference of Arrival (A-TDOA) have been proposed for mitigating the synchronization error of the clocks of the architecture sensors. However, this architecture presents some drawbacks with regards to its synchronous base architecture Time Difference of Arrival (TDOA).

A-TDOA relies on a single clock of a coordinator sensor for collecting the time measurements for avoiding the synchronization errors thus making the architecture more dependable on this sensor and the architecture less versatile. This inherent problem of the A-TDOA architecture could produce potential problems in failure conditions of the architecture making the A-TDOA less competitive than the TDOA architecture in these situations.

In this paper, we analyze the behavior of the TDOA and A-TDOA architecture in nominal and failure conditions. This requires the minimization of the system uncertainties in both conditions and the guarantee of the localization algorithm convergence in the minimum sensor configuration (4 nodes) in both architectures.

We guarantee the algorithm convergence through the consideration of the maximization of the convergence radius in all the possible coverage region and we first introduce the maximum convergence points for achieving full coverage in unexpected conditions, harsh coverage regions or initial time series iteration points.

Results show that the consideration of all these potential problems of the A-TDOA architecture during the optimization of the sensor distribution enables it to overcome the deficits of the architecture and therefore making it competitive for LPS applications. Particularly, in the two scenarios of simulations of this paper, A-TDOA supposes a reduction of the error bounds in 78.7% and 89.5% and increases in 86% and 33% the convergence radius with regards to the TDOA architecture. In addition, maximum convergence points are more easily found in the A-TDOA configuration which has been firstly studied in this paper. Therefore, higher refreshing rates of the positioning signal are allowed and higher accuracy is provided in the A-TDOA architecture showing this architecture as an optimal candidate for high-demanded accuracy applications in harsh environments.

CRediT authorship contribution statement

Javier Díez-González: Conceptualization, Investigation, Resources, Software, Writing – original draft. **Rubén Álvarez:** Conceptualization, Investigation, Resources, Software, Visualization, Writing – original draft. **Paula Verde:** Methodology, Resources, Validation, Writing – review & editing. **Rubén Ferrero-Guillén:** Formal analysis, Validation, Writing – review & editing. **Hilde Perez:** Formal analysis, Project administration, Supervision, Validation, Writing – review & editing.

Declaration of Competing Interest

The authors declare that they have no known competing financial interests or personal relationships that could have appeared to influence the work reported in this paper.

Acknowledgements

This research has been developed and funded by the project of the Spanish Ministry of Science and Innovation grant number PID2019-108277GB-C21.

References

[1] D.S. Deif, Y. Gadallah, Classification of wireless sensor networks deployment techniques, IEEE Commun. Surv. Tutorials 16 (2) (2014) 834–855, https://doi.org/10.1109/SURV.2013.091213.00018.
[2] E. Xu, Z. Ding, S. Dasgupta, Source localization in wireless sensor networks from signal time-of-arrival measurements, IEEE Trans. Signal Process. 59 (6) (2011) 2887–2897, https://doi.org/10.1109/TSP.2011.2116012.
[3] X. Li, Collaborative localization with received-signal strength in wireless sensor networks, IEEE Trans. Veh. Technol. 56 (6) (2007) 3807–3817, https://doi.org/10.1109/TVT.2007.904535.
[4] I. Shames, A.N. Bishop, M. Smith, B.D. Anderson, Doppler shift target localization, IEEE Trans. Aerosp. Electron. Syst. 49 (1) (2013) 266–276, https://doi.org/10.1109/TAES.2013.6404102.
[5] P. Kulakowski, J. Vales-Alonso, E. Egea-López, W. Ludwin, J. García-Haro, Angle-of-arrival localization based on antenna arrays for wireless sensor networks, Comput. Electr. Eng. 36 (6) (2010) 1181–1186, https://doi.org/10.1016/j.compeleceng.2010.03.007.
[6] Y. Zhang, L. Duan, A phase-difference-of-arrival assisted ultra-wideband positioning method for elderly care, Measurement 170 (2021) 108689, https://doi.org/10.1016/j.measurement.2020.108689.
[7] F. Zhang, Y. Sun, Q. Wan, Calibrating the error from sensor position uncertainty in TDOA-AOA localization, Signal Process. 166 (2020) 107213, https://doi.org/10.1016/j.sigpro.2019.07.006.
[8] J. Diez-Gonzalez, R. Alvarez, H. Perez, Optimized cost-effective node deployments in asynchronous time local positioning systems, IEEE Access 8 (2020) 154671–154682, https://doi.org/10.1109/Access.628763910.1109/ACCESS.2020.3018624.
[9] I. Guvenc, C.C. Chong, A survey on TOA based wireless localization and NLOS mitigation techniques, IEEE Commun. Surv. Tutorials 11 (3) (2009) 107–124, https://doi.org/10.1109/SURV.2009.090308.
[10] Z. Zhang, F. Jiang, B. Li, A novel time difference of arrival localization algorithm using a neural network ensemble model, Int. J. Distributed Sensor Networks 14 (11) (2018) 1-12. doi: 10.1177/1550147718815798
[11] O. Jean, A.J. Weiss, Passive localization and synchronization using arbitrary signals, IEEE Trans. Signal Process. 62 (8) (2014) 2143–2150, https://doi.org/10.1109/TSP.2014.2307281.
[12] S. He, X. Dong, High-accuracy localization platform using asynchronous time difference of arrival technology, IEEE Trans. Instrum. Meas. 66 (7) (2017) 1728–1742, https://doi.org/10.1109/TIM.2017.2666278.
[13] R. Alvarez, J. Diez-Gonzalez, P. Verde, H. Perez, Comparative performance analysis of time local positioning architectures in NLOS urban scenarios, IEEE Access 8 (2020) 225258–225271, https://doi.org/10.1109/Access.628763910.1109/ACCESS.2020.3044389.
[14] K. Yang, J. An, X. Bu, G. Sun, Constrained total least-squares location algorithm using time-difference-of-arrival measurements, IEEE Trans. Veh. Technol. 59 (3) (2010) 1558–1562, https://doi.org/10.1109/TVT.2009.2037509.
[15] J. Díez-González, R. Álvarez, L. Sánchez-González, L. Fernández-Robles, H. Perez, M. Castejón-Limas, 3D Tdoa problem solution with four receiving nodes, Sensors 19 (13) (2019) 2892, https://doi.org/10.3390/s19132892.
[16] X. Chen, D. Wang, J. Yin, Y. Wu, Performance analysis and dimension-reduction Taylor series algorithms for locating multiple disjoint sources based on TDOA under synchronization clock bias, IEEE Access 6 6 (2018) 48489–48509, https://doi.org/10.1109/ACCESS.2018.2860958.
[17] B. Jin, X. Xu, T. Zhang, Robust time-difference-of-arrival (TDOA) localization using weighted least squares with cone tangent plane constraint, Sensors 18 (3) (2018) 778, https://doi.org/10.3390/s18030778.
[18] J. Díez-González, R. Álvarez, P. Verde, R. Ferrero-Guillén, D. González-Bárcena, H. Perez, Stable Performance Under Sensor Failure of Local Positioning Systems, International Workshop on Soft Computing Models in Industrial and Environmental Applications, Burgos, Castilla y León, Spain (2020). doi: 10.1007/978-3-030-57802-2_48
[19] R. Kaune, Accuracy studies for TDOA and TOA localization, 2012 15th International Conference on Information Fusion, Singapour (2012). doi:
[20] Y. Begriche, M. Thameri, K. Abed-Meraim, Exact conditional and unconditional Cramér-Rao bounds for near field localization, Digital Signal Process. 31 (2014) 45–58, https://doi.org/10.1016/j.dsp.2014.04.006.
[21] M.u. Zhou, Y. Wang, Y. Liu, Z. Tian, An Information-Theoretic View of WLAN Localization Error Bound in GPS-Denied Environment, IEEE Trans. Veh. Technol. 68 (4) (2019) 4089–4093, https://doi.org/10.1109/TVT.2510.1109/TVT.2019.2896482.
[22] W. Zhang, G. Han, X. Wang, M. Guizani, K. Fan, L. Shu, A node location algorithm based on node movement prediction in underwater acoustic sensor networks, IEEE Trans. Veh. Technol. 69 (3) (2020) 3166–3178, https://doi.org/10.1109/TVT.2510.1109/TVT.2019.2963406.
[23] J. Díez-González, R. Álvarez, D. González-Bárcena, L. Sánchez-González, M. Castejón-Limas, H. Perez, Genetic algorithm approach to the 3D node localization in TDOA systems, Sensors 19 (18) (2019) 3880, https://doi.org/10.3390/s19183880.
[24] J. Díez-González, R. Álvarez, N. Prieto-Fernández, H. Perez, Local wireless sensor networks positioning reliability under sensor failure, Sensors 20 (5) (2020) 1426, https://doi.org/10.3390/s20051426.
[25] N.-T. Nguyen, B.-H. Liu, The mobile sensor deployment problem and the target coverage problem in mobile wireless sensor networks are NP-Hard, IEEE Syst. J. 13 (2) (2019) 1312–1315, https://doi.org/10.1109/JSYST.426700310.1109/JSYST.2018.2828879.
[26] R.V. Kulkarni, G.K. Venayagamoorthy, Particle swarm optimization in wireless-sensor networks: a brief survey, IEEE Trans. Syst., Man, Cybern. Part C (Applications and Reviews) 41 (2) (2011) 262–267, https://doi.org/10.1109/TSMCC.2010.2054080.
[27] C.S. Shieh, V.O. Sai, Y.C. Lin, T.F. Lee, T.T. Nguyen, Q.D. Le, Improved Node Localization for WSN Using Heuristic Optimization Approaches, in: 2016 International Conference on Networking and Network Applications (NaNA), 2016, https://doi.org/10.1109/NaNA.2016.58.
[28] D. Moreno-Salinas, A. Pascoal, J. Aranda, Sensor networks for optimal target localization with bearings-only measurements in constrained three-dimensional scenarios, Sensors 13 (8) (2013) 10386–10417, https://doi.org/10.3390/s130810386.
[29] R. alvarez, J. Diez-Gonzalez, L. Sanchez-Gonzalez, H. Perez, Combined noise and clock CRLB error model for the optimization of node location in time positioning systems, IEEE Access 8 (2020) 31910–31919, https://doi.org/10.1109/Access.628763910.1109/ACCESS.2020.2973709.
[30] I. Landa-Torres, S. Gil-Lopez, S. Salcedo-Sanz, J. Del Ser, J.A. Portilla-Figueras, A novel grouping harmony search algorithm for the multiple-type access node location problem, Expert Syst. Appl. 39 (5) (2012) 5262–5270, https://doi.org/10.1016/j.eswa.2011.11.013.
[31] G.P. Gupta, S. Jha, Biogeography-based optimization scheme for solving the coverage and connected node placement problem for wireless sensor networks, Wireless Networks 25 (6) (2019) 3167–3177, https://doi.org/10.1007/s11276-018-1709-0.
[32] F. Domingo-Perez, J.L. Lazaro-Galilea, A. Wieser, E. Martin-Gorostiza, D. Salido-Monzu, A. De la Llana, Sensor placement determination for range-difference positioning using evolutionary multi-objective optimization, Expert Syst. Appl. 47 (2016) 95–105, https://doi.org/10.1016/j.eswa.2015.11.008.
[33] A. Al-Qaisi, A.I. Alhasanat, A. Mesleh, B.S. Sharif, C.C. Tsimenidis, J.A. Neasham, Quantized lower bounds on grid-based localization algorithm for wireless sensor networks, Ann. Telecommun. 71 (5-6) (2016) 239–249, https://doi.org/10.1007/s12243-016-0494-y.
[34] V.H.S. de Abreu, P.H. González, G.R. Mauri, G.M. Ribeiro, R.D. Orrico, N.F.R. Campos Júnior, C.A. Abramides, Network sensor location problem with monitored lanes: Branch-and-cut and clustering search solution techniques, Comput. Ind. Eng. 150 (2020) 106827, https://doi.org/10.1016/j.cie.2020.106827.
[35] R. Ferrero-Guillén, J. Díez-González, P. Verde, R. Álvarez, H. Perez, Table organization optimization in schools for preserving the social distance during the COVID-19 pandemic, Appl. Sci. 10 (23) (2020) 8392, https://doi.org/10.3390/app10238392.
[36] A. Efrat, S. Har-Peled, J. S. B. Mitchell, Approximation algorithms for two optimal location problems in sensor networks, 2nd International Conference on Broadband Networks, Boston, Massachussetus, USA (2005). doi: 10.1109/ICBN.2005.1589677.
[37] X. Wang, J.J. Ma, S. Wang, D.W. Bi, Distributed particle swarm optimization and simulated annealing for energy-efficient coverage in wireless sensor networks, Sensors 7 (5) (2007) 628–648, https://doi.org/10.3390/s7050628.
[38] H.M. Kanoosh, E.H. Houssein, M.M. Selim, Salp swarm algorithm for node localization in wireless sensor networks, J. Comput. Networks Commun. 2019 (2019) 1–12, https://doi.org/10.1155/2019/1028723.
[39] J. Díez-González, P. Verde, R. Ferrero-Guillén, R. Álvarez, H. Perez, Hybrid memetic algorithm for the node location problem in local positioning systems, Sensors 20 (19) (2020) 5475, https://doi.org/10.3390/s20195475.
[40] P. Verde, J. Díez-González, R. Ferrero-Guillén, A. Martínez-Gutiérrez, H. Perez, Memetic chains for improving the local wireless sensor networks localization in urban scenarios, Sensors 21 (2021) 2458, https://doi.org/10.3390/s21072458.
[41] K. Kannadasan, D.R. Edla, M.C. Kongara, V. Kuppili, M-Curves path planning model for mobile anchor node and localization of sensor nodes using Dolphin Swarm Algorithm, Wireless Netw. 26 (4) (2020) 2769–2783, https://doi.org/10.1007/s11276-019-02032-4.
[42] R. V. Kulkarni, G. K. Venayagamoorthy, M. X. Cheng, Bio-inspired node localization in wireless sensor networks, 2009 IEEE International Conference on Systems, Man and Cybernetics, San Antonio, Texas, USA (2009). doi: 10.1109/ICSMC.2009.5346107.
[43] Z. Wang, H. Xie, Z. Hu, D. Li, J. Wang, W. Liang, Node coverage optimization algorithm for wireless sensor networks based on improved grey wolf optimizer, J. Algor. Comput. Technol. 13 (2019) 1–15, https://doi.org/10.1177/1748302619889498.
[44] N. N. Qin, J. L. Chen, An area coverage algorithm for wireless sensor networks based on differential evolution, Int. J. Distrib. Sensor Networks 14 (8) (2018) 1-11.
[45] S.D. Correia, M. Beko, L.A. Da Silva Cruz, S. Tomic, Elephant herding optimization for energy-based localization, Sensors 18 (9) (2018) 2849, https://doi.org/10.3390/s18092849.

[46] J. Bhola, S. Soni, G.K. Cheema, Genetic algorithm based optimized leach protocol for energy efficient wireless sensor networks, J. Ambient Intell. Humanized Comput. 11 (3) (2020) 1281–1288, https://doi.org/10.1007/s12652-019-01382-3.

[47] R. Alvarez, J. Diez-Gonzalez, N. Strisciuglio, H. Perez, Multi-objective optimization for asynchronous positioning systems based on a complete characterization of ranging errors in 3D complex environments, IEEE Access 8 (2020) 43046–43056, https://doi.org/10.1109/Access.628763910.1109/ACCESS.2020.2978336.

[48] A. Ouyang, Y. Lu, Y. Liu, M. Wu, X. Peng, An Improved Adaptive Genetic Algorithm based on DV-Hop for Locating Nodes in Wireless Sensor Networks, Neurocomputing (2021) In Press. doi: 10.1016/j.neucom.2020.04.156

[49] M.L. Ruz, J. Garrido, J. Jiménez, R. Virrakoski, F. Vázquez, Simulation tool for the analysis of cooperative localization algorithms for wireless sensor networks, Sensors 19 (13) (2019) 2866, https://doi.org/10.3390/s19132866.

[50] M. Kowalski, P. Willett, T. Fair, Y. Bar-Shalom, CRLB for estimating time-varying rotational biases in passive sensors, IEEE Trans. Aerosp. Electron. Syst. 56 (1) (2020) 343–355, https://doi.org/10.1109/TAES.710.1109/TAES.2019.2917992.

[51] R. Kaune, J. Hörst y W. Köch, Accuracy analysis for TDOA localization in sensor networks, 14th International Conference on Information Fusion, Chicago, Illinois, USA (2011).

[52] T. S. Rappaport, Wireless Communications, Upper Saddle River: Prentice Hall, Principles and Practice.

[53] Abdulmalik Shehu Yaro, Ahmad Zuri Sha'ameri, Effect of path loss propagation model on the position estimation accuracy of a 3-dimensional minimum configuration multilateration system, Int. J. Integrated Eng. 10 (4) (2018), https://doi.org/10.30880/ijie10.30880/ijie.2018.10.0410.30880/ijie.2018.10.04.006.

[54] R. Ferrero-Guillén, J. Díez-González, R. Álvarez, H. Perez, Analysis of the Genetic Algorithm Operators for the Node Location Problem in Local Positioning Systems, International Conference on Hybrid Artificial Intelligence Systems (HAIS 2020), Gijón, Asturias, Spain (2020). doi: 10.1007/978-3-030-61705-9_23.

Javier Díez-Gonzalez was born in León, Spain in 1994. He received the B.S. degree in aerospace engineering in 2016, the M.S. degree in aeronautical engineering, and the Ph.D. degree in 2020 from the University of León and the M.S. in Artificial Intelligence from the International University of Valencia in 2021. He has also followed the leadership program of the University Francisco de Vitoria (Madrid) where he graduated in 2017. His research interests are the optimization of manufacturing processes, sensor location in LPS, industry 4.0 and the applied artificial intelligence. He is currently a Researcher within the Department of Mechanical, Computer and Aerospace Engineering at the University of León where he is working as a lecturer in the area of Mechanics.

Rubén Álvarez was born in León, Spain in 1994. He received the B.S. degree in aerospace engineering in 2016, the M.S. degree in aeronautical engineering in 2018 and the Ph.D. degree in 2020 from the University of León and the M.S. in Artificial Intelligence from the International University of Valencia in 2019. His research focus is on the optimization of LPS sensor location for high accuracy applications and Natural Language Processing. He is currently a Researcher within the Department of Mechanical, Computer and Aerospace Engineering at the University of León where he is developing a positioning system for high-accuracy navigation of autonomous vehicles.

Paula Verde was born in León, Spain in 1994. He earned the B.S. degree in software engineering from the University of León in 2016 and the M.S. in Telecommunications from the University Oberta of Cataluña in 2021. She has also finished the grant of Network programming, DEVNET, from Cisco Networking Academy. She is now pursuing the Ph.D. degree at the University of León. In her professional career she has been part of the University Institute for Automatics and Manufacturing promoting the Drotium startup. Her research interests include communication networks, artificial intelligence and localization. She is currently a Researcher within the Department of Mechanical, Computer and Aerospace Engineering at the University of León.

Rubén Ferrero-Guillén was born in Valencia, Spain, in 1998. He received the B.S. degree in aerospace engineering from the University of León in 2020. He is now pursuing the Master's Degree in aeronautical engineering in the University of León, while also working for the Ph.D. degree. He is currently a Researcher within the Department of Mechanical, Computer and Aerospace Engineering, University of León, working with the area of mechanics. His research interests are the applied optimization and LPS architectures.

Hilde Perez is Associate Professor and Head of the Department of Mechanical, Computer and Aerospace Engineering at the University of León. She received her engineering degree in Mechanical Engineering from the University of Oviedo and in Electrical and Electronic Engineering from the University of León. She received her Ph. D. from Polytechnic University of Madrid in 2012. She has been involved in different national research projects in collaboration with the Polytechnic University of Madrid. The research areas of interest are related with Industry 4.0, smart systems for manufacturing, Automated Guided Vehicles, Localization and Collaborative Robots.